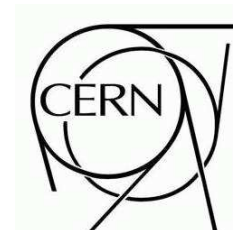




ATLAS NOTE

ATL-COM-TILECAL-2008-010

August 27, 2008



Effects of ATLAS Tile calorimeter failures on jets and missing transverse energy measurements

P. Mermod¹, G. Arabidze², D. Milstead¹ and R. Stanek³

¹*Stockholm University, Sweden*

²*University of Athens, Greece*

³*Argonne National Laboratory, USA*

Abstract

Failures of the ATLAS Tile calorimeter would affect the jet energy resolution and would fake tails of missing transverse energy. Significant effects are expected in processes involving high transverse momentum jets ($p_T > 100$ GeV). These effects, their consequences, as well as methods to minimize them, are studied using simulated data for various degradation topologies and for different physics processes.

1 Introduction

Studies of physics processes at the LHC presently rely on simulated data. Simulations of the detector include intrinsic performance effects due to, e.g., cracks or miscalibration [1]. However, simulated data usually do not take into account accidental hot or dead channels (or even whole dead regions) in the detectors. Such detector failures might substantially affect the measurement precision or the discovery potential in a physics analysis. In particular, an accurate measurement of the missing transverse energy (\cancel{E}_T), which relies on the calorimeters, is crucial in many physics searches [2].

In this paper, the impact of a failing ATLAS Tile (hadronic) Calorimeter (TileCal) is investigated in some detail. In a recent cosmic ray data study [3], it has been shown that noisy cells in the calorimeters can induce large amounts of fake \cancel{E}_T . In the present study, we assume that hot or noisy cells are identified and masked, and consider only the effects of dead cells in TileCal. Trigger issues are not considered here.

This paper is organized as follows : descriptions of the MC processes and of the TileCal degradation topologies used for the study are given in sections 2 and 3 ; a discussion of the relative fraction of jet energy deposited in TileCal is presented in section 4 ; results on the effects of TileCal degradation on jets and \cancel{E}_T are presented and discussed in sections 5 and 6 ; and a summary and conclusions are given in section 7.

2 MC Samples

The MC data used in this paper passed through a full ATLAS simulation¹⁾. Three different physics channels were considered ; they are listed below with the corresponding MC models in parenthesis :

- $t\bar{t}$ (MC@NLO, considering all decays except all-hadronic)
- J5 (Pythia, QCD processes with $280 < \hat{p}_T < 560$ GeV)
- J7 (Pythia, QCD processes with $1120 < \hat{p}_T < 2240$ GeV)

The $t\bar{t}$ process is an important source of background in many analyses, and is also a very interesting standard model process in itself. The J5 and J7 processes are important when studying very high- p_T physics. They are used here as benchmarks to quantify the effects of a failing TileCal on jets and \cancel{E}_T measurements.

3 Scenarios

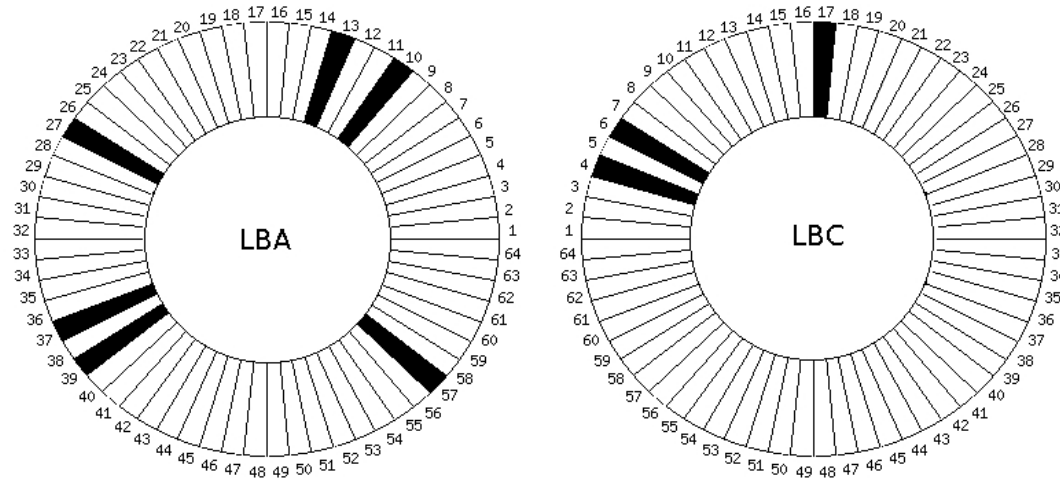
Six illustrative TileCal degradation topologies have been considered (for a complete description of TileCal, see, e.g., [4]) :

- No degradation.
- Whole TileCal off.
- 9 disabled drawers²⁾ at random in the long barrels³⁾. This scenario is illustrated in Fig. 1(a).

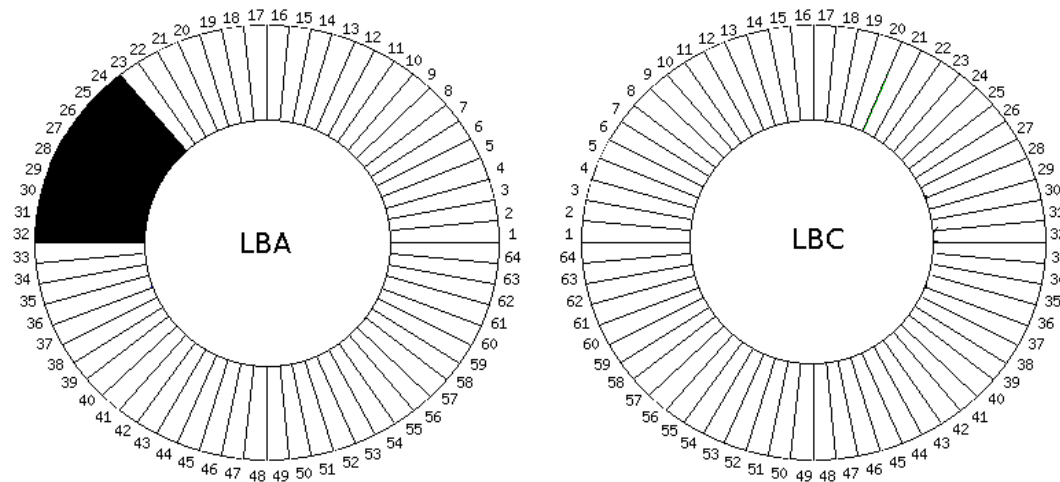
¹⁾The data were reconstructed with Athena release 12.0.31. The jet definition was *Cone4TowerParticleJets*, with a cone radius of 0.4, Pt of seeds of 1 GeV, and a split/merge fraction of 0.5 ; the towers were made on the EM scale and calibrated with a global H1 algorithm. The \cancel{E}_T definition was *MET_Final*, with calibrated cell energies in topoclusters (H1 algorithm) and taking into account muons (Moore algorithm) and cryostat corrections (from Kt jets).

²⁾There are 64 drawers in total for each TileCal barrel.

³⁾The TileCal long barrels LBA and LBC cover the pseudorapidity range $0 < |\eta| < 0.9$.



(a) 9 modules at random in the long barrels



(b) 9 contiguous modules in LBA

Figure 1: Drawing of the TileCal modules in the long barrels LBA and LBC. The modules shown in black correspond to the nine disabled drawers in the scenarios considered for the present study.

- 144 disabled DMUs⁴⁾ at random in the long barrels (only J7).
- 9 contiguous disabled drawers in the long barrel (only J7). This scenario is illustrated in Fig. 1(b).
- 9 disabled drawers at random in the extended barrels⁵⁾ (only J7).

The extreme case where the whole TileCal is disabled gives us an idea of the role played by the hadronic calorimeter in different physics cases. Nine whole drawers turned off at random positions in the long barrels (LB) is a quite pessimistic scenario, but not unrealistic. We might also have a certain amount of bad channels (e.g., noisy PM tubes) distributed over the whole barrel ; to illustrate this, here we consider 144 DMUs - the equivalent of 9 drawers in number of channels - at random in the LB. We consider also the failure of 9 contiguous drawers ⁶⁾ : in this case, we expect larger amounts of \cancel{E}_T , as the undetected part of the hadronic showers tends to act in the same direction. Finally, with the last scenario, we study the extended barrels (EB). We will discuss further the implications of these different situations in section 6.

4 The non-electromagnetic fraction

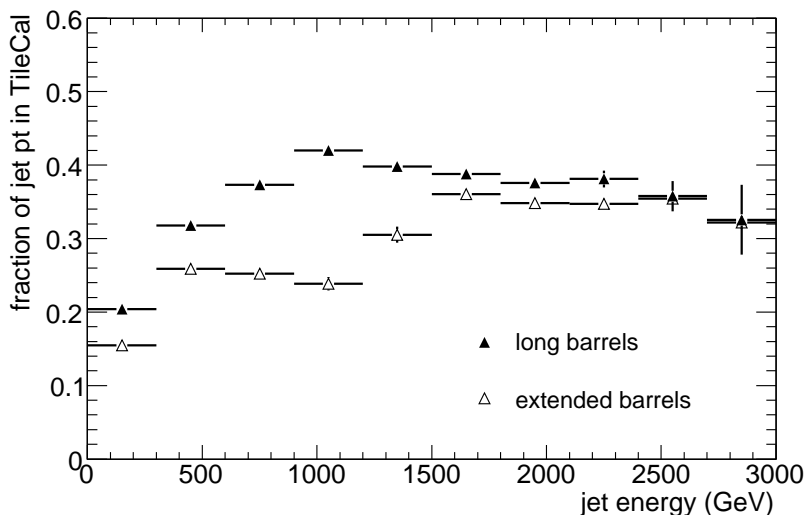


Figure 2: Profile histogram showing the mean fraction of jet p_T in TileCal as a function of the jet energy. The η regions corresponding to the LB and EB are plotted as closed and open triangles, respectively. Both the J5 and J7 processes were used to produce this figure.

The profile histograms plotted in Fig. 2 show the mean fraction of transverse energy deposited in TileCal as a function of the jet energy. The fraction of energy in TileCal is seldom greater than 40% since most of the shower is captured by the LAr electromagnetic calorimeter [5].

As expected, this fraction increases with the jet energy as the shower penetrates deeper into the calorimeters. However, there are non-linearities. In the LB ($|\eta| < 0.9$, black triangles), the fraction

⁴⁾The DMUs are part of the TileCal drawer digitizers. There are 16 DMUs in each drawer, each of them serving 3 channels.

⁵⁾The TileCal extended barrels EBA and EBC cover the pseudorapidity range $0.9 < |\eta| < 1.7$.

⁶⁾For instance, the failure of a 200 V power supply with a spare channels would switch off 8 contiguous drawers ; there are other failures which can take down individual drawers.

flattens around 1000 GeV and even starts to decrease a bit for very high jet energies. For the EB ($0.9 < |\eta| < 1.7$, open triangles), we observe two plateaux. This behavior predicted by the MC might not reproduce real data accurately, as the way very energetic hadronic showers develop in the calorimeters is currently based on models which have been tested experimentally only with pion test beams [5]. But jets behave very differently from single pions, as 300 GeV pions would release much more energy in TileCal than 300 GeV jets, for instance [4]. The amount of electromagnetic calorimeter material and dead material is larger in the EB region [5], and consequently, for the EB, we see, on average, about 5 to 10% less energy deposited in TileCal.

5 Effects on jet resolution

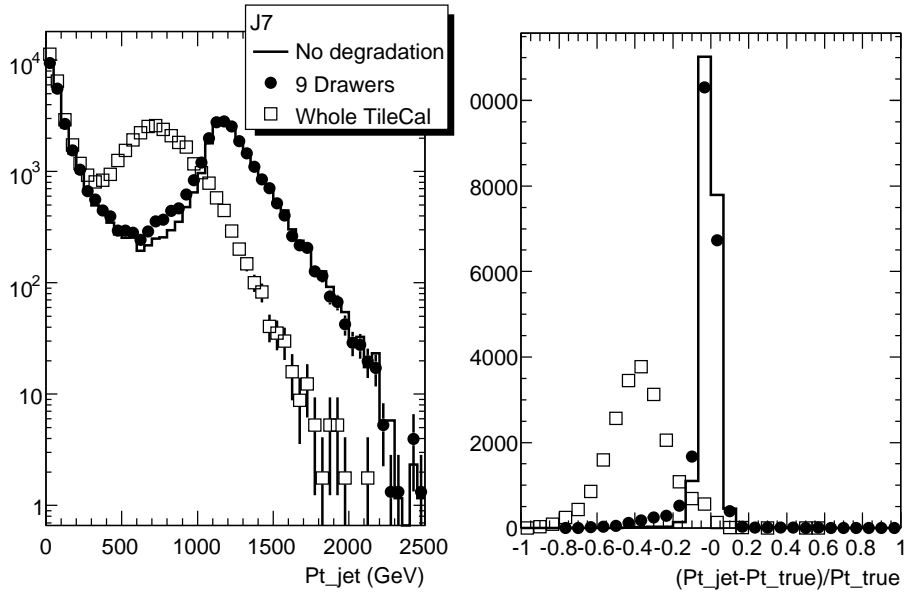


Figure 3: Jet p_T distribution (left panel) and jet p_T resolution (right panel) for J7. The solid line corresponds to no degradation, the black dots to 9 randomly failed drawers, and the open squares to the whole TileCal off. The plots are normalized to 10000 events.

As discussed in the previous section, TileCal is expected to account for at most for 40% of the jet p_T measurement for high- p_T jets. The J7 process was used to produce Fig. 3, where the maximal effect is seen by comparing the open squares (TileCal disabled) with the solid line (fully operational TileCal). The right panel of the figure shows the relative difference to the true jet p_T . The peak is shifted by about 0.02 when disabling 9 Drawers in the LB (black dots), and the width of the distribution gets larger by about 0.01. A shift of the peak by roughly 2% is expected from this simple argument : considering the long barrels only (which leads to a slight overestimation of the overall effect), 9 drawers correspond to $9/128=7\%$ of the detector, and 40% of the energy is expected to go undetected for jets in the corresponding regions ; this gives on average $0.07 \times 0.4 = 2.8\%$ less detected energy. In the scenario where the 9 drawers are in the EB (not shown in the figure), the shift is only about half a percent.

6 Effects on missing transverse energy

A mismeasurement of the jet energy when the jet falls into a dead calorimeter region can cause large amounts of fake \cancel{E}_T . In this section, we will look at \cancel{E}_T tails for different degradation topologies, investigate how the fake \cancel{E}_T depends on the jet η and p_T , and discuss possible remedies.

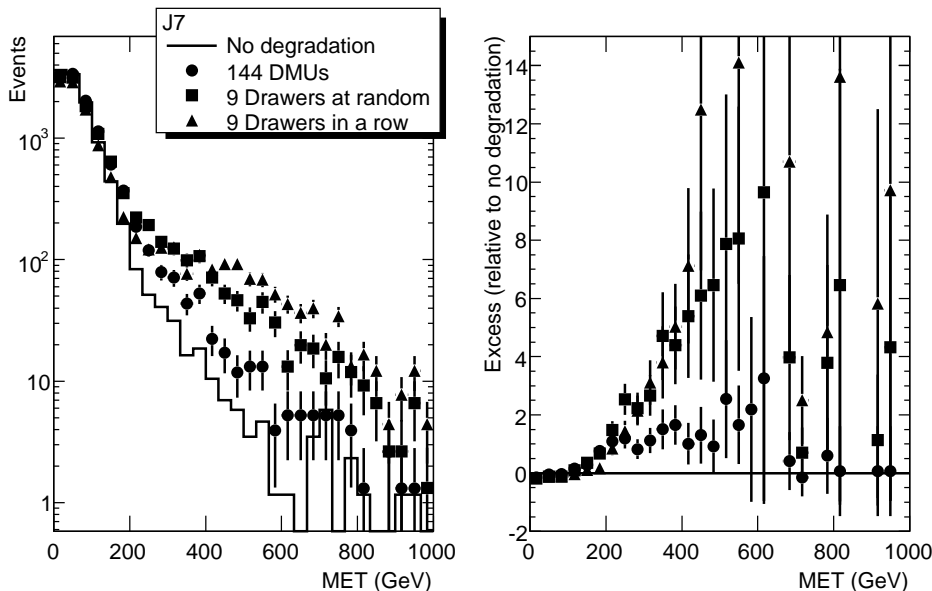


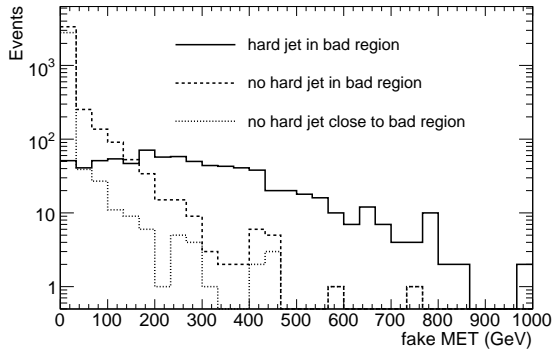
Figure 4: \cancel{E}_T distribution (left) and relative difference in the number of events with and without degradation as a function of \cancel{E}_T (right) for J7. The solid line corresponds to no degradation, the dots to 144 DMUs, the squares to 9 drawers and the triangles 9 contiguous drawers (always in LB). The plots are normalized to 10000 events.

The left panel of Fig. 4 shows \cancel{E}_T distributions for the J7 sample and various scenarios. The three degradations correspond to the same amount of dead channels ⁷⁾ (always in LB), but with decreasing homogeneity (from DMUs spread over the whole barrels to several contiguous drawers). We see that the \cancel{E}_T tails get more important as the bad channels get more concentrated in the same region of TileCal. In the right panel, we see by how much the number of events increases : up to a factor 10 for large \cancel{E}_T when 9 drawers are disabled, and by about 100% above 200 GeV in the case of 144 dead DMUs. Whether this is a problem or not in a real physics analysis depends, e.g., on the expected background contribution from hard QCD jets.

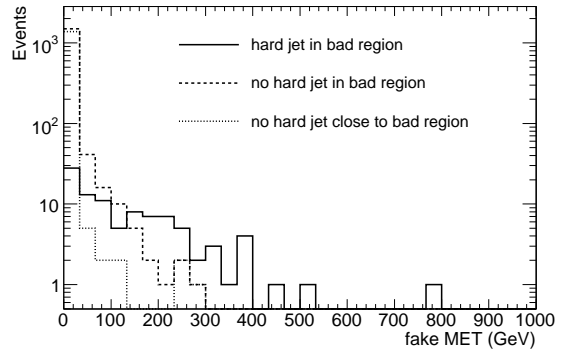
For the J5 sample (not shown in the figure), the effect is not as pronounced : we get about 100% more events for $\cancel{E}_T > 100$ GeV for 9 randomly failed drawers.

For the $t\bar{t}$ sample (not shown in the figure), disabling 9 drawers does not cause significant changes in the \cancel{E}_T distribution. There are two reasons for the $t\bar{t}$ process to have little sensitivity to disabling parts of TileCal : the jet energy is, on average, less than 100 GeV, which means that little of it is measured by TileCal (see Fig. 2) ; and there are anyway relatively large amounts of natural \cancel{E}_T coming from physics, which dilutes the effects of instrumental \cancel{E}_T considered here. However, this last argument does not apply for the all-hadronic $t\bar{t}$ process, which is not considered in the present study.

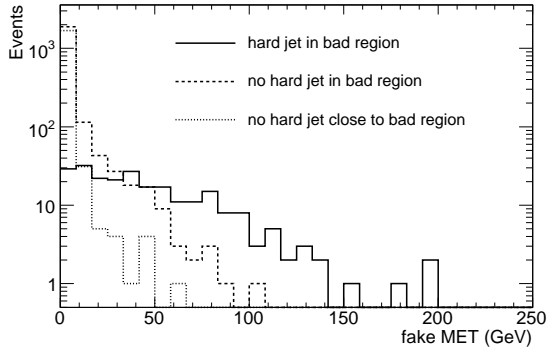
⁷⁾Although the degradation effects on the reconstruction performance are different : if only one of the two channels corresponding to the same scintillator is switched off, the energy is corrected by doubling the output of the other channel ; this



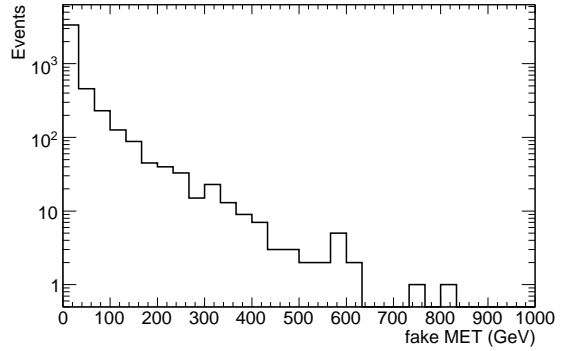
(a) J7, 9 drawers in the long barrels



(b) J7, 9 drawers in the extended barrels



(c) J5, 9 drawers in the long barrels



(d) J7, 144 DMUs in the long barrels

Figure 5: Fake \cancel{E}_T distributions. Solid line : at least one hard jet in the dead region. Dashed line : no hard jet in the dead region. Dotted line : no hard jet in the dead region extended by 0.1 in eta and phi (corresponds to excluding also adjacent drawers).

Fake \cancel{E}_T ⁸⁾ distributions are shown in Fig. 5. For the solid lines, a selection was made requiring at least one hard jet ($p_T > 500$ GeV for J7 and $p_T > 150$ GeV for J5) to fall inside a dead region. For J7 with 9 dead drawers in the LB (Fig. 5(a)), these events exhibit an average fake \cancel{E}_T of 270 GeV. If we consider the same dead drawers in the EB (still J7, Fig. 5(b)), the average value is 130 GeV. For J5 (9 drawers in LB, Fig. 5(c)), the average fake \cancel{E}_T with jets falling in the bad region is 50 GeV.

The fake \cancel{E}_T can be greatly reduced by rejecting events containing hard jets in the bad regions (dashed lines), and even further by also rejecting events with hard jets in drawers adjacent to the dead ones (dotted lines), since the same jet might spread over several TileCal modules. But this is at the cost of efficiency : with 9 dead drawers in the LB, we lose 11% of the events with the first, tight rejection, and 32% with the second, looser one⁹⁾. Also, we see that even when the degraded regions are very well defined and vetoed, there is still some fake \cancel{E}_T . This is probably due to low-energy jets or jets which are reconstructed with low energy (or not reconstructed at all) due to the lack of Tile calorimeter information. Remember that we exclude only events with hard jets in the bad regions. We can imagine that if the LAr calorimeter was also failing in the same region, there would be very little information telling us if there were a jet there. In such a case, one would have to be very careful with events with a large \cancel{E}_T in the direction of the dead zone in the calorimeters. It would also introduce a bias for events containing true (physical) \cancel{E}_T .

In the case where we have many dead channels spread over the whole TileCal LB (Fig. 5(d)), the fake \cancel{E}_T due to TileCal degradation extends up to several hundreds GeV for J7, with about 10% of the events with a fake \cancel{E}_T greater than 50 GeV and about 2% above 200 GeV¹⁰⁾. This can probably not be trivially reduced.

7 Summary and conclusion

Various TileCal degradation scenarios were investigated, and the effect on jet energy measurement and its repercussions on the \cancel{E}_T measurement were studied.

A jet falling into a completely dead TileCal region would be seen with 20-40% less transverse momentum on average, the effect being most important for high-energy and central jets. The changes in terms of jet resolution are not significant, but the resulting fake \cancel{E}_T is a serious issue.

If there are whole malfunctioning TileCal drawers, the fake \cancel{E}_T can be almost completely reduced by rejecting events with hard jets falling near to the corresponding TileCal modules, but this is at the cost of detector acceptance. In case there are many small dead spots to deal with, it is necessary to take into account the irreducible \cancel{E}_T tails in the analysis. The typical state of TileCal will be known while taking data. The overall behavior of fake \cancel{E}_T may not depend on the details of the actual degradation topology, thus hopefully allowing to run the Monte-Carlo reconstruction only once with a typical topology.

8 Acknowledgements

Many thanks to C. Clement, L. Fiorini and J. Proudfoot for their interest and good ideas.

happens more often for 144 DMUs than for 9 drawers.

⁸⁾In this work, fake \cancel{E}_T means the difference in \cancel{E}_T relative to no TileCal degradation (for the same events being reconstructed in different scenarios). It does not include the fake \cancel{E}_T already present without adding any degradation.

⁹⁾These numbers come from the study, they are not clear from the figure only.

¹⁰⁾Idem.

References

- [1] ATLAS Collaboration, ATLAS Detector and Physics Performance Technical Design Report, CERN/LHCC99-14 **1** (1999) 261.
- [2] Naoko Kanaya, SUSY Physics with Early Data : Understanding the ATLAS Detector and the Backgrounds, CP903, SUSY06, 14th International Conference **1** (2007) 201.
- [3] R.J. Teuscher et al., Fake Missing Transverse Energy from ATLAS Calorimeter Cosmic Ray Data, ATL-CAL-2008-002 (2008).
- [4] ATLAS Collaboration, Tile Calorimeter Technical Design Report, CERN/LHCC96-42 (1996).
- [5] ATLAS Collaboration, Calorimeter Performance Technical Design Report, CERN/LHCC96-40 (1997).